Journal of VLSI Signal Processing 30, 273–291, 2002

Adaptive Interference Suppression for the Downlink of a Direct Sequence CDMA System with Long Spreading Sequences*

COLIN D. FRANK
Advanced Radio Technology Group, Global Telecommunications Solution Sector, Motorola, 1501 W. Shure Drive, IL27-3G6, Arlington Heights, IL 60004, USA

EUGENE VISOTSKY
Communication Systems and Technologies Labs, Motorola Labs, Schaumburg, IL 60196, USA

UPAMANYU MADHOW†
Department of Electrical and Computer Engineering, University of California, Santa Barbara, CA 93106, USA

Received October 30, 2000; Revised July 2, 2001

Abstract. A simple approach for adaptive interference suppression for the downlink (base-to-mobile link) of a direct sequence (DS) based cellular communication system is presented. The base station transmits the sum of the signals destined for the different mobiles, typically attempting to avoid intra-cell interference by employing orthogonal spreading sequences for different mobiles. However, the signal reaching any given mobile passes through a dispersive channel, thus destroying the orthogonality. In this paper, we propose an adaptive linear equalizer at the mobile that reduces interference by approximately restoring orthogonality. The adaptive equalizer uses the pilot's spreading sequence (which observes the same channel as the spreading sequence for the desired mobile) as training. Simulation results for the linear Minimum Mean Squared Error (MMSE) equalizer are presented, demonstrating substantial performance gains over the RAKE receiver. Long spreading sequences (which vary from symbol to symbol) are employed, so that the equalizer adapts not to the time-varying spreading sequences, but to the slowly varying downlink channel. Since the inter-cell interference from any other base station also has the structure of many superposed signals passing through a single channel, the adaptive equalizer can also suppress inter-cell interference, with the tradeoff between suppression of intra- and inter-cell interference and noise enhancement depending on their impact on the Mean Squared Error (MSE).

Keywords: CDMA, MMSE, equalization, adaptive, multi-user detection

1. Introduction

IS-95, the second generation US digital cellular standard, is based on direct sequence (DS) code division multiple access (CDMA), in which each user uses all of the available bandwidth, with different *spreading* sequences being employed to distinguish between different users. Worldwide third generation cellular standards also appear to have converged on DS-CDMA. The primary traffic on present day cellular networks is voice, so that the forward link or downlink (base-to-mobile) and the reverse link or uplink (mobile-to-base) carry similar traffic volumes. However, in the near future, the downlink is expected to carry significantly

*Part of this work was presented at the 36th Annual Allerton Conference on Communication, Control and Computing, Monticello, Illinois, September 1998.

†The work of U. Madhow was supported in part by the National Science Foundation under grant NCR96-24008 (CAREER) and by the Army Research Office under grant DAAD19-00-1-0567.

more traffic due to applications such as web browsing by mobile terminals. The downlink is therefore expected to be the bottleneck in traditional cellular architectures, which currently allocate equal bandwidth resources to both the uplink and downlink. Even for the current cellular telephony applications, the uplink has several advantages over the downlink: uplink power control eliminates the near-far problem, whereas downlink power control leads to a possible near-far problem *by design* (since the base transmits at higher power to mobiles who are further away, multipath components for the signal destined for such users can seriously impact reception at a mobile close to the base station); receiver processing can be more sophisticated at the base for the uplink than at the mobile for the downlink. Interference suppression at the mobile receiver appears to be an attractive method of enhancing the downlink, since the small number of interfering sources (the neighboring base stations), together with the information available from the pilot signal, present some practical opportunities for improvement.

In IS-95 as well as proposed CDMA-based third generation standards, the downlink is designed to be free of intra-cell interference under ideal conditions. The base station transmits the sum of the signals destined for the different mobiles in the cell, with orthogonal spreading sequences assigned to different mobiles. Of course, this orthogonality is destroyed when the signal passes through a multipath channel, leading to intra-cell interference. The key idea in this paper is to equalize the channel at the mobile receiver, thus approximately restoring the orthogonality among the spreading sequences and reducing the interference. The problem is exactly analogous to that of equalization of a narrowband system, except that the chips now play the role of symbols. In a given chip interval, the base station transmits the sum of the chips (times the symbols) destined for each user, together with the chip for the pilot sequence. All elements in this sum observe the same channel, so that, for the linear equalization strategy considered here, an equalizer for the pilot sequence works for the desired user as well. The pilot sequence can therefore play the role of a perpetual training sequence for adaptive equalization. The adaptation is based on the linear MMSE criterion.

The idea of equalizing the downlink channel for the purpose of restoring orthogonality of the user spreading sequences was first proposed in [1]. There a block equalizer is developed for a hybrid time division CDMA system. Equalization of the downlink for a DS-CDMA system was first independently introduced in [2], [3] and [4]. In [2], an MMSE solution for the downlink equalizer of a CDMA system is computed. The use of orthogonal spreading sequences, however, is not considered. In [3], an adaptive MMSE equalizer is presented, while [4] considers its zero-forcing counterpart. Equalization of the downlink has subsequently been proposed in numerous other works, such as [5–11] to name a few. See also the paper by T.P. Krauss, W.J. Hillery, and M.D. Zoltowski in this journal issue.

The idea of restoring orthogonality on the downlink through the use of equalization is especially useful since it leads to an adaptive receiver performing interference suppression even for CDMA systems with no spreading code periodicities. In [3], an adaptive algorithm for training the downlink equalizer is developed based on the pilot training sequence. A very similar algorithm was proposed later in [10]. An adaptive algorithm not requiring the pilot training sequence is proposed in [7]. Finally, an adaptive reduced-rank equalizer for sparse downlink channels is introduced in [12].

The rest of this paper is organized as follows. Section 2 introduces the system model. Section 3 develops the basic MMSE chip equalizer designed to equalize the downlink channel. This equalizer is a function of the user spreading sequences, and hence time-variant and computationally complex. A time-invariant version of the MMSE chip equalizer, denoted the average MMSE chip equalizer, is derived in Section 3. A symbol-level implementation of the average MMSE chip equalizer, amenable to adaptive implementation, is proposed in Section 4. Simulation results illustrating the performance of the adaptive receiver in a variety of channel conditions are shown in Section 5. Finally, conclusions are presented in Section 6.

Throughout this paper, $\mathbf{a}^T$, $\mathbf{a}^*$, $\mathbf{a}^H = (\mathbf{a}^*)^T$, denote transpose, conjugate and hermitian transpose of vector $\mathbf{a}$, respectively.

2. System Model

Since the proposed equalization technique mitigates inter- as well as intra-cell interference, we consider a two base station model in this paper. However, for simplicity of exposition, we first explain the structure of the signals transmitted from a single base station. The discussion is then extended to accommodate multiple base stations by using superscripts to index the different base stations.

Consider a given cell. The base station simultaneously transmits data to the active users (or mobiles) in its cell, and transmissions to all users are symbol-synchronous. To facilitate channel estimation in the mobile, the base station also transmits a synchronous pilot signal. The users and the pilot are assigned distinct spreading sequences which enables the mobile to separate the pilot signal and the desired transmission from multiple access interference. In IS-95, every base-station is assigned a unique complex spreading sequence $s_b(n)$, where n indexes the chip time. All spreading sequences within the cell are derived from this basic spreading sequence. Let us consider this operation in detail. Each user, including the pilot, is assigned an orthogonal Walsh code of length N, with the all-ones Walsh code reserved for the pilot. Let $w_k(n)$ denote the Walsh code for user k, expressed as a periodic sequence of period N, with $w_k(n) = w_k(n+N)$ for all n. Letting $\mathbf{w}_k = [w_k(0), \ldots, w_k(N-1)]^T$ denote the Walsh code for user k over a symbol period as an N-length vector, we have, due to orthogonality of the Walsh codes over a symbol period, that $\mathbf{w}_k^T \mathbf{w}_j = N\delta(j-k)$, where $\delta(\cdot)$ is the delta function. Over each symbol interval, the user's spreading sequence is generated by multiplying the corresponding Walsh code and the base station's spreading sequence. That is,

$$s_k(n) = s_b(n) w_k(n) \quad 1 \le k \le K$$

where K is the number of simultaneous users in the cell. Denoting the pilot as user with subscript 0, we also have that

$$s_0(n) = s_b(n) w_0(n) = s_b(n)$$

since $w_0(n) \equiv 1$, for all n. Note that the spreading sequences for different users, including the pilot, inherit the orthogonality of the Walsh codes over each symbol interval. The base station's (or pilot's) spreading sequence $s_0(n)$ itself is a *long* complex spreading sequence of period much larger than N, and is well modeled as aperiodic with random independent and identically distributed components, with $E\{s_0(n)\} = 0$. Note that, under this model, any user's spreading sequence can be determined from knowledge of the pilot's spreading code and the particular Walsh code being used by the user. The equalization method proposed here applies both to the preceding *orthogonal spreading* model, or to a *random spreading* model in which the $s_k(n)$ are modeled as independent and identically distributed for different k and n, such that $E\{s_k(n)\} = 0$. Furthermore, under both models we have

$$\begin{aligned} E\{s_k(n) s_k^*(m)\} &= E\left\{|s_k(n)|^2\right\}\delta(n-m) \\ E\{s_k(n) s_k(m)\} &= 0 \end{aligned} \tag{1}$$

for all k, n and m.

Let $b_k(n)$ denote the symbol sequence for mobile k, expressed at the chip rate. Thus, $b_k(n)$ is piecewise constant over symbol intervals of length N chips, where N denotes the processing gain. That is, the lth symbol sent by user k is given by

$$b_k(n) = b_k(lN) \quad lN \le n \le (l+1)N - 1$$

Letting P_k denote the transmit power assigned to user k, we obtain that $u_k(n) = \sqrt{P_k}\, s_k(n) b_k(n)$ is the net transmitted sequence, expressed at the chip rate, destined for that user. As noted above, we denote the pilot code as user 0, with $u_0(n) = \sqrt{P_0}\, s_0(n)$, since $b_0(n) \equiv 1$ (the pilot is unmodulated). The net chip rate transmitted sequence from the base station is therefore given by

$$u(n) = \sum_{k=0}^{K} u_k(n)$$

where K again denotes the total number of users transmitted by the base station, so that the total number of traffic channels utilized by the base station, including the pilot channel, is $K+1$. Since the spreading sequences for different users are orthogonal over each symbol interval, it is possible to recover the symbols without incurring intra-cell interference by despreading over a symbol interval. Thus, the despreader output $\sum_{n=lN}^{(l+1)N-1} s_k^*(n) u(n)$ is proportional to the lth symbol of user k.

The complex baseband signal transmitted from the base station is given by

$$\sum_{n=-\infty}^{\infty} u(n) \psi(t - nT_c)$$

where $\frac{1}{T_c}$ is the chip rate, and $\psi(t)$ is the chip waveform. In IS-95, the Fourier transform $\Psi(f)$ of the chip waveform is roughly square root raised cosine at the chip rate. Ideally, $\Psi(f)$ would be chosen as square root Nyquist at the chip rate. Typically, the receive filter is also chosen as a square root Nyquist pulse so that the composition of the transmit and receive filters is

Nyquist at the chip rate, thus eliminating inter-chip interference in channels with no multipath. In this case, the transmitted sequence $u(n)$ would be recovered by sampling at the chip rate, and the symbol-level orthogonality of the $s_k(n)$ would then permit recovery of the symbols $b_k(n)$ without incurring intra-cell interference.

In practice, the channel to the desired mobile is dispersive, leading to inter-chip, and hence intra-cell, interference. The output of the receive filter is therefore typically sampled faster than the chip rate (say at a rate of n_o/T_c, where n_o is the oversampling factor). For implementing the RAKE receiver, the delays of the significant multipath components of the channel are estimated (typically with a resolution of T_c/n_o), and maximal-ratio combining is performed. For simplicity, however, we consider a *chip rate* discrete-time channel model in this paper. For a time-invariant channel, the chip-rate sequence at the output of the receive filter is given by the convolution of the chip-rate transmitted sequence with the chip-rate discrete time channel to the desired mobile, plus interference and noise.

2.1. Two Base Station Model

The notation for this model is as before, except for the addition of a superscript identifying the base station. The received sequence $r(n)$ is given by

$$r(n) = \left(u^{(1)} * h^{(1)}\right)(n) + \left(u^{(2)} * h^{(2)}\right)(n) + n(n) \quad (2)$$

where $(a * b)(n)$ denotes the convolution between sequences $\{a(n)\}$ and $\{b(n)\}$. For $i = 1, 2$, $\{u^{(i)}(n)\}$ is the chip rate sequence transmitted by base station i, and $\{h^{(i)}(n)\}$ is the channel from base station i to the desired mobile. Finally, $\{n(n)\}$ is the additive noise, which accounts for the interference from distant cells as well as receiver thermal noise. To obtain (2), synchronization at the chip rate among the two base stations is assumed. Synchronization is assumed only for notational convenience and has no effect on either the implemenation or the performance of the receiver. Due to the interference averaging effect of CDMA, the noise is well modeled as White Gaussian Noise (WGN) of variance $N_0/2$ per dimension. Note that under this system model there are two types of other-cell interference impinging on the desired cell: non-white interference from the adjacent base station given by the second summand in (2), and white interference from distant base stations included in the noise term of (2). This distinction is necessary since linear equalization is capable of suppressing only non-white interference. Detailed results on the suppression capabilities of non-white other-cell interference are presented in Section 4.3.

It is convenient to normalize the channels from the two base stations by absorbing the channel gains into the power of the transmitted sequences $\{u^{(i)}(n)\}$, $i = 1, 2$, so that

$$\sum_{n=-\infty}^{\infty} \left|h^{(1)}(n)\right|^2 = \sum_{n=-\infty}^{\infty} \left|h^{(2)}(n)\right|^2 = 1$$

Without loss of generality, let the desired mobile have index 1 and be served by base station 1. Consistent with IS-95 terminology, we refer to the total power received by the mobile from the desired base station as I_{or} and the total power received by the mobile from the other base station as I_{oc}. That is,

$$I_{or} = E\left[\left|u^{(1)}(n)\right|^2\right] = \sum_{k=0}^{K^{(1)}} P_k^{(1)}$$

and

$$I_{oc} = E\left[\left|u^{(2)}(n)\right|^2\right] = \sum_{k=0}^{K^{(2)}} P_k^{(2)}$$

where $K^{(i)}$ denotes the number of mobiles in cell i.

3. Linear MMSE Equalization

As noted initially in [1], and subsequently for IS-95 spreading sequences in [3], the benefit of equalization on the forward link is greatly enhanced when orthogonal sequences are used to separate the different users. With orthogonal spreading sequences, the multiple-access intra-cell interference introduced by multipath is completely eliminated through the use of zero-forcing equalization, i.e. full inversion of the downlink channel. In order to minimize the noise enhancement associated with zero-forcing equalization and also to suppress non-white additive noise (such as that produced by other base stations), finite impulse response (FIR) MMSE equalization is used. The proposed receiver architecture is depicted in Fig. 1. Our objective is to estimate the chip rate sequence $\{u_1^{(1)}(n)\}$ (the desired signal), from which the desired symbol sequence is recovered by despreading using the desired spreading sequence $\{s_1^{(1)}(n)\}$.

Consider an arbitrary time index n. Consider a finite length equalizer, of length $L = L_1 + L_2 + 1$, that uses the block of samples $\mathbf{r}(n) = [r(n - L_1), \ldots, r(n-1), r(n), r(n+1), \ldots, r(n + L_2)]^T$ to estimate $u_1^{(1)}(n)$. The estimate, or the decision statistic, is

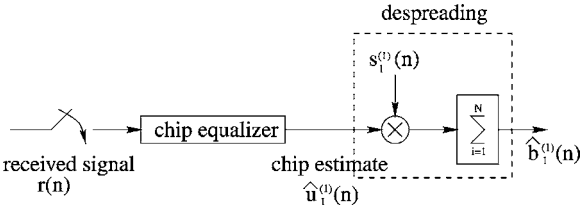

Figure 1. Conceptual diagram of the chip equalizer.

given by the complex inner product $\langle \mathbf{c}, \mathbf{r}(n) \rangle = \mathbf{c}^H \mathbf{r}(n)$. It is shown below that, in general, the MMSE equalizer of $u_1^{(1)}(n)$ is time-varying, i.e., a function of n.

Without loss of generality, the impulse responses from both base stations are assumed to have finite support on the interval $[M_1, M_2]$. With this assumption, the received vector $\mathbf{r}(n)$ can be written in matrix form as

$$\mathbf{r}(n) = \mathbf{H}^{(1)}\mathbf{u}^{(1)}(n) + \mathbf{H}^{(2)}\mathbf{u}^{(2)}(n) + \mathbf{n}(n) \qquad (3)$$

where $H^{(i)}$, $i = 1, 2$, is a matrix of dimension $(L_1 + L_2 + 1) \times (L_1 + L_2 + 1 + M_2 - M_1)$, of the form

$$\mathbf{H}^{(i)} = \begin{bmatrix} h^{(i)}(M_2) & h^{(i)}(M_2 - 1) & \cdots & h^{(i)}(M_1) & 0 & \cdots & 0 \\ 0 & h^{(i)}(M_2) & \cdots & h^{(i)}(M_1 + 1) & h^{(i)}(M_1) & 0 & \cdots \\ \vdots & \vdots & \vdots & \vdots & \vdots & \vdots & \vdots \\ 0 & \cdots & 0 & h^{(i)}(M_2) & \cdots & h^{(i)}(M_1 + 1) & h^{(i)}(M_1) \end{bmatrix}$$

and the vectors $\mathbf{u}^{(1)}(n)$ and $\mathbf{u}^{(2)}(n)$ have dimension $L_1 + L_2 + 1 + M_2 - M_1$ and are given by

$$\mathbf{u}^{(i)}(n) = \left[u^{(i)}(n - L_1 - M_2), u^{(i)}(n - L_1 - M_2 + 1), \ldots, u^{(i)}(n + L_2 - M_1)\right]^T$$

The expression for the MMSE estimate of the desired user's signal at time n, $u_1^{(1)}(n)$, from the observation $\mathbf{r}(n)$ is given by [13]

$$\hat{u}_1^{(1)}(n) = \left(\mathbf{c}_1^{(1)}(n)\right)^H \mathbf{r}(n)$$

where

$$\mathbf{c}_1^{(1)}(n) = (E_s\{\mathbf{r}(n)\mathbf{r}^H(n)\})^{-1} E_s\left\{\mathbf{r}(n)\left(u_1^{(1)}(n)\right)^*\right\}$$

and E_s denotes the expectation over the user symbols and noise, conditioned on the user spreading sequences $\{s_k^{(i)}(n), i = 1, 2; 1 \le k \le K^{(i)}\}$.

Let the length $L_1 + L_2 + 1$ vector $\boldsymbol{\mu}_1^{(1)}(n)$ be defined as

$$\boldsymbol{\mu}_1^{(1)}(n) \equiv E_s\left\{\mathbf{r}(n)\left(u_1^{(1)}(n)\right)^*\right\}$$

If the user symbols are independent and identically distributed, so that

$$E\left\{b_k^{(i)}(l) b_m^{(j)}(n)\right\} = \delta(i - j)\delta(k - m)\delta(\lfloor l/N \rfloor - \lfloor n/N \rfloor)$$

where $\lfloor \cdot \rfloor$ denotes the floor operation, then the p-th element of the expectation vector $\boldsymbol{\mu}_1^{(1)}(n)$ can be written as

$$\mu_{1,p}^{(1)}(n) = \sqrt{P_1^{(1)}} \sum_{l=M_1}^{M_2} h^{(1)}(l) s_1^{(1)}(n - L_1 + p - l) \times \left(s_1^{(1)}(n)\right)^* \delta\left(\left\lfloor \frac{n - L_1 + p - l}{N} \right\rfloor - \left\lfloor \frac{n}{N} \right\rfloor\right) \qquad (4)$$

for $0 \le p \le L_1 + L_2$.

Let $\boldsymbol{\Theta}(n)$ denote the $L_1 + L_2 + 1 \times L_1 + L_2 + 1$ correlation matrix, given by

$$\boldsymbol{\Theta}(n) \equiv E_s\{\mathbf{r}(n)\mathbf{r}^H(n)\} = \mathbf{H}^{(1)}\mathbf{U}^{(1)}(n)\left(\mathbf{H}^{(1)}\right)^H + \mathbf{H}^{(2)}\mathbf{U}^{(2)}(n)\left(\mathbf{H}^{(2)}\right)^H + N_0\mathbf{I}_{L_1+L_2+1}$$

where

$$\mathbf{U}^{(i)}(n) = E_s\left\{\mathbf{u}^{(i)}(n)\left(\mathbf{u}^{(i)}(n)\right)^H\right\} \quad i = 1, 2$$

and $\mathbf{I}_k$ is the $k \times k$ identity matrix.

The matrix $\mathbf{U}^{(i)}(n)$ is a square matrix of dimension $L_1 + L_2 + 1 + M_2 - M_1$, and has elements

$$U_{l,m}^{(i)}(n) = E_s\left\{u^{(i)}(n - L_1 - M_2 + l) \times \left(u^{(i)}(n - L_1 - M_2 + m)\right)^*\right\} \qquad (5)$$

for $0 \le l, m \le L_1 + L_2 + M_2 - M_1$ and 0 else. If, as assumed above, the user symbol sequences are independent and identically distributed, the expectation in (5) can be computed as follows

$$E_s\{u^{(i)}(m)(u^{(i)}(n))^*\} = \sum_{j=0}^{K^{(i)}} P_j^{(i)} s_j^{(i)}(m)(s_j^{(i)}(n))^* \times \delta\left(\left\lfloor \frac{m}{N} \right\rfloor - \left\lfloor \frac{n}{N} \right\rfloor\right) \quad (6)$$

To summarize the above development, the MMSE equalizer for $u_1^{(1)}(n)$ from the observation $\mathbf{r}(n)$ is given by

$$\mathbf{c}_1^{(1)}(n) = \left(E_s\{\mathbf{r}(n)\mathbf{r}^H(n)\}\right)^{-1} E_s\left\{\mathbf{r}(n)\left(u_1^{(1)}(n)\right)^*\right\} = (\boldsymbol{\Theta}(n))^{-1}\boldsymbol{\mu}_1^{(1)}(n) \quad (7)$$

Because the correlation matrix $\boldsymbol{\Theta}(n)$ and the mean vector $\boldsymbol{\mu}_1^{(1)}(n)$ are functions of the chip index n, the MMSE equalizer is also a function of the index n. In fact, if the spreading sequences are periodic with a period P divisible by N (as in IS-95), the correlation matrix, the mean vector, and the equalizer in (7) all have period P also.

As a result of the above, the equalizer in (7) has the following properties, when applied at mobile j, served by base station i.

1. The mean vector, $\boldsymbol{\mu}_j^{(i)}(n)$, depends on the base station index i, the user index j, and the chip index n. Consequently, the mean vector cannot be measured as a time average, and must be computed for each chip index n. Calculation of the mean requires knowledge of the desired user's spreading sequence $\{s_j^{(i)}(n)\}$ and power $P_j^{(i)}$, as well as the channel impulse response from the base station of interest.
2. The correlation matrix $\boldsymbol{\Theta}(n)$ also changes with the chip index n. As a result, the correlation matrix cannot be measured as a time average. Instead, $\boldsymbol{\Theta}(n)$ and its inverse must be computed anew for each chip index n. This computation requires knowledge of the channel matrices $\mathbf{H}^{(1)}$ and $\mathbf{H}^{(2)}$, and the set of spreading sequences and user amplitudes used by both base stations.

It is apparent that the MMSE chip equalizer is computationally very complex and depends on detailed parameters of the transmitted signal. Furthermore, a new chip equalizer must be recomputed for each chip index n, which renders its implementation, under current complexity constraints, impractical. For this reason, it is useful to define an average MMSE chip equalizer, which will be shown to be both substantially less complex and amenable to adaptive implementation.

3.1. Average MMSE Chip Equalizer

We define the *average* MMSE chip equalizer of $u_1^{(1)}(n)$ from observation $\mathbf{r}$ as

$$\bar{\mathbf{c}}_1^{(1)} \equiv (E\{E_s\{\mathbf{r}(n)\mathbf{r}^H(n)\}\})^{-1} E\left\{E_s\left\{\mathbf{r}(n)\left(u_1^{(1)}(n)\right)^*\right\}\right\} \equiv \bar{\boldsymbol{\Theta}}^{-1}\bar{\boldsymbol{\mu}}_1^{(1)} \quad (8)$$

where the outer expectations average over the user spreading sequences. At first glance, it is reasonable to expect that the final expression for the average MMSE chip equalizer depends upon whether the random or orthogonal spreading model is used to compute the required expectations. However, we now show that this is not the case.

From (4) and (6), it is apparent that the instantaneous MMSE chip equalizer depends on the user spreading sequences only through auto-correlations. But from (1) the statistical auto-correlation properties under both spreading models of interest are the same. Hence, the average MMSE chip equalizer is the same. In particular, by taking the expectations in (4) and (6), it is straightforward to show that under both spreading models, we have

$$\bar{\boldsymbol{\mu}}_1^{(1)} = \sqrt{P_1^{(1)}}\,\mathbf{h}^{(1)} \quad (9)$$

where $\mathbf{h}^{(i)} = [h^{(i)}(-L_1), h^{(i)}(-L_1+1), \ldots, h^{(i)}(L_2)]^T$, and

$$\bar{\boldsymbol{\Theta}} = I_{or}\mathbf{H}^{(1)}\left(\mathbf{H}^{(1)}\right)^H + I_{oc}\mathbf{H}^{(2)}\left(\mathbf{H}^{(2)}\right)^H + N_0\mathbf{I}_{L_1+L_2+1}$$

In summary, the average MMSE estimate of $u_1^{(1)}(n)$ from the observation $\mathbf{r}(n)$ is given by $(\bar{\mathbf{c}}_1^{(1)})^H\mathbf{r}(n)$, where

$$\bar{\mathbf{c}}_1^{(1)} = \sqrt{P_1^{(1)}}\,\bar{\boldsymbol{\Theta}}^{-1}\mathbf{h}^{(1)} \quad (10)$$

Note that, within a multiplicative constant, the average MMSE chip equalizer is the same for all users transmitted from base station one. Furthermore, because the correlation matrix $\bar{\boldsymbol{\Theta}}$ does not depend on the base station of interest, the average MMSE chip equalizer for the second base station is given by simply replacing $\mathbf{h}^{(1)}$ with $\mathbf{h}^{(2)}$ in (10).

The average MMSE chip equalizer can be calculated directly from the knowledge of channels $\mathbf{h}^{(1)}$ and $\mathbf{h}^{(2)}$, from which channel matrices $\mathbf{H}^{(1)}$ and $\mathbf{H}^{(2)}$ can be computed, the sum powers received from the serving and interfering base stations, I_{or} and I_{oc}, and the noise spectral density N_0. The channels can be estimated, within a positive multiplicative constant, by time-averaging $(s_0^{(1)}(n))^*\mathbf{r}(n)$ and $(s_0^{(2)})^*\mathbf{r}(n)$, and the average signal correlation matrix can be estimated as the time-average of $\mathbf{r}(n)\mathbf{r}^H(n)$. As a result, the complexity associated with direct computation of the average MMSE chip equalizer is not unreasonable.

3.2. SIR Expressions

Consider an arbitrary (time-varying) linear estimate $\mathbf{v}^H(n)\mathbf{r}(n)$ used to estimate $u_1^{(1)}(n)$ from the observation $\mathbf{r}(n)$. A standard performance measure for the estimator $\mathbf{v}(n)$ is the signal-to-interference ratio (SIR) of the estimate $\mathbf{v}^H(n)\mathbf{r}(n)$, which is defined as the ratio of the desired signal energy to the interference variance. That is, for $\mathbf{v}^H(n)\mathbf{r}(n)$ the SIR is given by

$$SIR(n) \equiv \frac{\left|E_s\left\{\mathbf{v}^H(n)\mathbf{r}(n)\left(u_1^{(1)}(n)\right)^*\right\}\right|^2}{E_s\{\mathbf{v}^H(n)\mathbf{r}(n)\mathbf{r}^H(n)\mathbf{v}\} - \left|E_s\left\{\mathbf{v}^H(n)\mathbf{r}(n)\left(u_1^{(1)}(n)\right)^*\right\}\right|^2} = \frac{\left|\mathbf{v}^H(n)\boldsymbol{\mu}_1^{(1)}(n)\right|^2}{\mathbf{v}^H(n)\boldsymbol{\Theta}(n)\mathbf{v}(n) - \left|\mathbf{v}^H(n)\boldsymbol{\mu}_1^{(1)}(n)\right|^2}$$

where the expectations are taken over the user symbol sequences, conditioned on user spreading sequences. For the optimum time-varying chip equalizer in (7), this expression simplifies to the following

$$SIR_{chip}(n) = \frac{\left(\boldsymbol{\mu}_1^{(1)}(n)\right)^H(\boldsymbol{\Theta}(n))^{-1}\boldsymbol{\mu}_1^{(1)}(n)}{1 - \left(\boldsymbol{\mu}_1^{(1)}(n)\right)^H(\boldsymbol{\Theta}(n))^{-1}\boldsymbol{\mu}_1^{(1)}(n)} \quad (11)$$

Note that the equalizer and, consequently, the SIR expression are time-varying. More specifically, the mean-square energy, the noise variance, and the ratio of these two quantities are periodic in the chip index n.

Consistent with the time-invariant structure of the average MMSE chip equalizer in (8), we define a time-invariant average SIR performance measure for this equalizer as the ratio of the average desired signal energy to the average interference variance, where the averaging is performed over the user spreading sequences as well the user symbols. That is,

$$\overline{SIR}_{chip} \equiv \frac{\left|\left(\bar{\mathbf{c}}_1^{(1)}\right)^H\bar{\boldsymbol{\mu}}_1^{(1)}\right|^2}{\left(\bar{\mathbf{c}}_1^{(1)}\right)^H\bar{\boldsymbol{\Theta}}\bar{\mathbf{c}}_1^{(1)} - \left|\left(\bar{\mathbf{c}}_1^{(1)}\right)^H\bar{\boldsymbol{\mu}}_1^{(1)}\right|^2} = \frac{P_1^{(1)}\left(\mathbf{h}^{(1)}\right)^H\bar{\boldsymbol{\Theta}}^{-1}\mathbf{h}^{(1)}}{1 - P_1^{(1)}\left(\mathbf{h}^{(1)}\right)^H\bar{\boldsymbol{\Theta}}^{-1}\mathbf{h}^{(1)}}$$

4. Symbol-Level Implementation of the Equalizer

The low complexity average MMSE equalizer (8) is well suited for stationary channels, in which the equalizer parameters are time-invariant and a single set of the equalizer coefficients can be precomputed and reapplied. In dynamic situations, where computation of the equalizer coefficients in real time is not possible due to complexity constraints, an adaptive implementation of the equalizer is desirable. However, although time-invariant, the average chip equalizer in (8) is not well suited for adaptive implementation. An adaptive implementation of the chip equalizer would adapt using the pilot's signal or the desired user's signal, which, for heavily loaded systems, are training signals with a very low SIR. As described in [3], to resolve this problem, the despreading operation can be directly incorporated into the equalization cost function, which enables (i) adaptive implementation of the equalizer using the training signal at a higher SIR, (ii) direct estimation of the desired user's symbols, rather than chips. We refer to this approach as *symbol-level* equalization. Hence, in contrast to the chip-level equalizers, for which the objective is to estimate the chip sequence for the user of interest, the objective of the symbol-level equalizer is to directly estimate the symbols of the user of interest. The basic functional diagram of the symbol-level equalizer, shown in Fig. 2, is similar to that of the chip equalizer. The distinction is that the chip equalizer measures the equalization error at the chip rate, prior to the despreader, whereas the symbol-level equalizer measures the error after the despreading and integration, at the symbol rate. Note that the equalizer coefficients are fixed for the duration of the

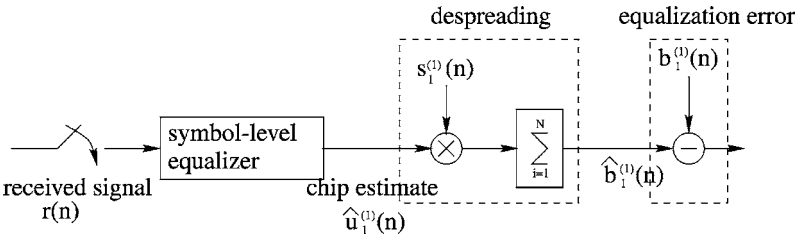

Figure 2. Conceptual diagram of the pre-despreading implementation of the symbol-level equalizer.

symbol period. In general, the equalizer coefficients can be time-varying from symbol to symbol.

Two implementations of the symbol-level equalizer are possible. In a conceptually simplified implementation shown in Fig. 2, the symbol-level equalizer precedes the despreading operation (pre-despreading implemenation). The output of the equalizer is obtained at the chip rate and despread to arrive at the symbol estimate. For analytical purposes, it is convenient to consider the post-despreading implementation of the symbol level equalizer, where the despreading precedes equalization. Post-despreading implementation of the equalizer is shown in Fig. 3. As above, let the equalizer consist of $L_1 + L_2 + 1$ chip-spaced taps. For the j-th symbol of the desired user, $b_1^{(1)}(jN)$, the equalizer input is a vector of length $L_1 + L_2 + 1$ formed by correlating the received sequence, $\{r(n)\}$, with the spreading sequence of the user of interest, $\{s_1^{(1)}(n)\}$, over the chip index interval $[jN, (j+1)N-1]$, at each of the $L_1 + L_2 + 1$ tap positions within the span of the equalizer. Note that in this implementation, the equalizer is applied once per symbol, and the output of the equalizer is at symbol rate. If the same set of the equalizer coefficients is used for the pre- and post-despreading implementations, the equalizer yields the same output at symbol rate and, hence the MMSE solution for both symbol-level implementations is the same. We proceed with the post-despreading implementation to derive the optimum symbol-level equalizer.

Let $\mathbf{z}_1^{(1)}(j)$ denote the input vector to the equalizer corresponding to the j-th symbol of the desired user. As previously, the subscript denotes the user index and the superscript denotes the serving base station. The l-th element of this vector is given by

$$z_{1,l}^{(1)}(j) = \sum_{m=0}^{N-1} r(jN - L_1 + l + m)\left(s_1^{(1)}(jN+m)\right)^*$$

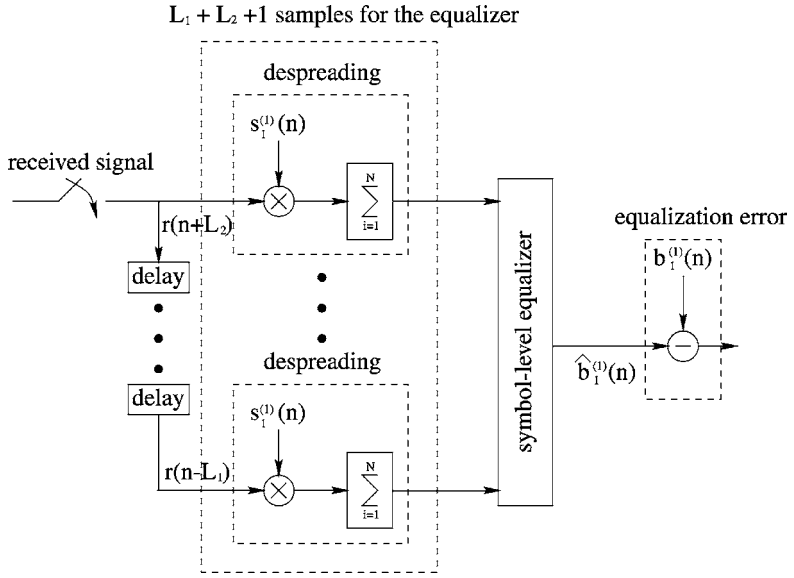

Figure 3. Conceptual diagram of the post-despreading implementation of the symbol-level equalizer.

where $0 \le l \le L_1 + L_2$. Using the matrix notation defined in (3), vector $\mathbf{z}_1^{(1)}(j)$ can be expressed in a compact form as follows

$$\begin{aligned}\mathbf{z}_1^{(1)}(j) &= \sum_{m=0}^{N-1} \mathbf{r}(jN+m)\big(s_1^{(1)}(jN+m)\big)^* \\ &= \mathbf{H}^{(1)} \sum_{m=0}^{N-1} \mathbf{u}^{(1)}(jN+m)\big(s_1^{(1)}(jN+m)\big)^* \\ &\quad + \mathbf{H}^{(2)} \sum_{m=0}^{N-1} \mathbf{u}^{(2)}(jN+m)\big(s_1^{(1)}(jN+m)\big)^* \\ &\quad + \sum_{m=0}^{N-1} \mathbf{n}(jN+m)\big(s_1^{(1)}(jN+m)\big)^* \qquad (12)\end{aligned}$$

Let $\mathbf{p}_1^{(1)}(j)$ denote the MMSE symbol-level equalizer for symbol $b_1^{(1)}(jN)$, which is given by

$$\begin{aligned}\mathbf{p}_1^{(1)}(j) &= \Big(E_s\big\{\mathbf{z}_1^{(1)}(j)\big(\mathbf{z}_1^{(1)}(j)\big)^H\big\}\Big)^{-1} \\ &\quad \times E_s\big\{\mathbf{z}_1^{(1)}(j)\big(b_1^{(1)}(jN)\big)^*\big\} \\ &\equiv \big(\mathbf{\Gamma}_1^{(1)}(j)\big)^{-1}\boldsymbol{\nu}_1^{(1)}(j) \qquad (13)\end{aligned}$$

and where $\mathbf{\Gamma}_1^{(1)}(j)$ and $\boldsymbol{\nu}_1^{(1)}(j)$ are defined implicitly. The MMSE estimate of the desired symbol $b_1^{(1)}(jN)$ is given by the inner product $\langle \mathbf{p}_1^{(1)}(j), \mathbf{z}_1^{(1)}(j)\rangle$. In general, the MMSE equalizer is time-varying and depends on both the user of interest and the particular symbol to be estimated. From (13), the expressions for the mean vector and the covariance matrix in (13) can be derived, similarly to Eqs. (4–6). Although such derivation does not involve any conceptual difficulties, the resulting expressions are quite involved and omitted for conciseness.

A time-invariant average symbol-level equalizer is obtained by performing averaging of the mean vector $\boldsymbol{\nu}_1^{(1)}(j)$ and covariance matrix $\mathbf{\Gamma}_1^{(1)}(j)$ in (13) over the user spreading sequences. Thus, the average symbol-level equalizer $\bar{\mathbf{p}}_1^{(1)}$ is given by

$$\bar{\mathbf{p}}_1^{(1)} = \big(E\big\{\mathbf{\Gamma}_1^{(1)}(j)\big\}\big)^{-1} E\big\{\boldsymbol{\nu}_1^{(1)}(j)\big\} \equiv \big(\bar{\mathbf{\Gamma}}_1^{(1)}\big)^{-1}\bar{\boldsymbol{\nu}}_1^{(1)} \qquad (14)$$

Since the user spreading sequences are orthogonal over a symbol period under the orthogonal spreading model and non-orthogonal under the random spreading model, the expression for the average covariance is different under the two spreading models. Nevertheless, as with the chip-level equalizer, the average symbol-level equalizer will be shown to be identical (within a non-negative multiplicative factor) under the two spreading models.

For the random spreading model, the average covariance matrix in (14) is given by

$$\begin{aligned}\bar{\mathbf{\Gamma}}_1^{(1)} &= N\big(I_{or}\mathbf{H}^{(1)}\big(\mathbf{H}^{(1)}\big)^H + I_{oc}\mathbf{H}^{(2)}\big(\mathbf{H}^{(2)}\big)^H \\ &\quad + N_0\mathbf{I}_{L_1+L_2+1}\big) + R_{rand}\mathbf{h}^{(1)}\big(\mathbf{h}^{(1)}\big)^H \qquad (15)\end{aligned}$$

where $R_{rand} = (N^2 - N)P_1^{(1)}$. For the orthogonal spreading model, (15) needs to be modified to account for the orthogonality of the user spreading sequences over a symbol period. In particular, we obtain

$$\begin{aligned}\bar{\mathbf{\Gamma}}_1^{(1)} &= N\big(I_{or}\mathbf{H}^{(1)}\big(\mathbf{H}^{(1)}\big)^H + I_{oc}\mathbf{H}^{(2)}\big(\mathbf{H}^{(2)}\big)^H \\ &\quad + N_0\mathbf{I}_{L_1+L_2+1}\big) + R_{orth}\mathbf{h}^{(1)}\big(\mathbf{h}^{(1)}\big)^H \qquad (16)\end{aligned}$$

where $R_{orth} = N^2 P_1^{(1)} - N I_{or}$. Hence, the covariance matrices under the two spreading models differ only by a rank one matrix. The mean vector is the same under the two spreading models and is given by

$$\bar{\boldsymbol{\nu}}_1^{(1)} = N\sqrt{P_1^{(1)}}\,\mathbf{h}^{(1)}$$

A key fact used in the derivation of (15) and (16) is that, under both spreading models employed here,

$$E\big\{\big(s_k^{(i)}\big)^2\big\} = 0$$

for all k and i (see (1)). Note that this property does not hold for real spreading sequences.

From (15) and (16), and with the use of the matrix inversion lemma [14], it can be shown that for both spreading models

$$\begin{aligned}\bar{\mathbf{p}}_1^{(1)} &= \frac{1}{NI_{or}}\left(1 - \frac{\big(\mathbf{h}^{(1)}\big)^H\big(\mathbf{\Omega}^{(1)}\big)^{-1}\mathbf{h}^{(1)}}{1+\alpha\big(\mathbf{h}^{(1)}\big)^H\big(\mathbf{\Omega}^{(1)}\big)^{-1}\mathbf{h}^{(1)}}\right) \\ &\quad \times \big(\mathbf{\Omega}^{(1)}\big)^{-1}\bar{\boldsymbol{\nu}}_1^{(1)} \qquad (17)\end{aligned}$$

where

$$\begin{aligned}\mathbf{\Omega}^{(1)} &= \mathbf{H}^{(1)}\big(\mathbf{H}^{(1)}\big)^H + \frac{I_{oc}}{I_{or}}\mathbf{H}^{(2)}\big(\mathbf{H}^{(2)}\big)^H \\ &\quad - \mathbf{h}^{(1)}\big(\mathbf{h}^{(1)}\big)^H + \frac{N_0}{I_{or}}\mathbf{I}_{L_1+L_2+1} \qquad (18)\end{aligned}$$

and

$$\alpha = N\frac{P_1^{(1)}}{I_{or}}$$

for the orthogonal spreading model and

$$\alpha = (N-1)\frac{P_1^{(1)}}{I_{or}} + 1$$

for the random spreading model.

4.1. Adaptive Implementation

We note the following properties of the average symbol-level equalizer:

1. The average symbol-level equalizer is the same, within a positive multiplicative constant, for the random and orthogonal spreading models.
2. Analogous to the average chip equalizer, within a positive multiplicative constant, the average symbol-level equalizer is the same for all users transmitted from the same base station.
3. Under both spreading models, the average symbol-level and chip-level equalizers are equal, within a positive multiplicative constant. More generally, the average symbol-level equalizer is the same regardless of the number of chips combined in the post-despreading implementation. This follows from (17) by noting that the equalizer is independent, within a positive multiplicative constant, of the processing factor N.

Properties two and three provide a great degree of flexibility to the adaptive implementation of the average symbol-level MMSE equalizer. *In particular, for an IS-95-type CDMA system, property two enables the equalizer to be trained using the pilot channel but to be used on any traffic channel originating from the same base station as the training pilot.* This is especially desirable for an IS-95-type system, where all base stations transmit continuous pilots, in a sense providing perpetual training sequence for the equalizer. A conceptual diagram of the proposed adaptive equalizer using the pilot for adaptation is shown in Fig. 4. To generate the symbol-level decision statistic, the output of the equalizer is despread over N chips using the desired user's spreading sequence. To facilitate training, the chip-rate output of the equalizer is despread over N_1 chips and compared with the pilot's transmitted sequence (a sequence of $+1$'s for our system model). The difference is then used as an error signal in standard adaptive algorithms, such as LMS or RLS [15]. In this implementation then, the equalizer coefficients are adjusted N/N_1 times per symbol. By property three, the average symbol-level MMSE equalizer is independent of N and N_1. Hence N_1 is a free parameter which provides additional flexibility to the adaptive implementation. In particular, it allows a trade-off between the speed of

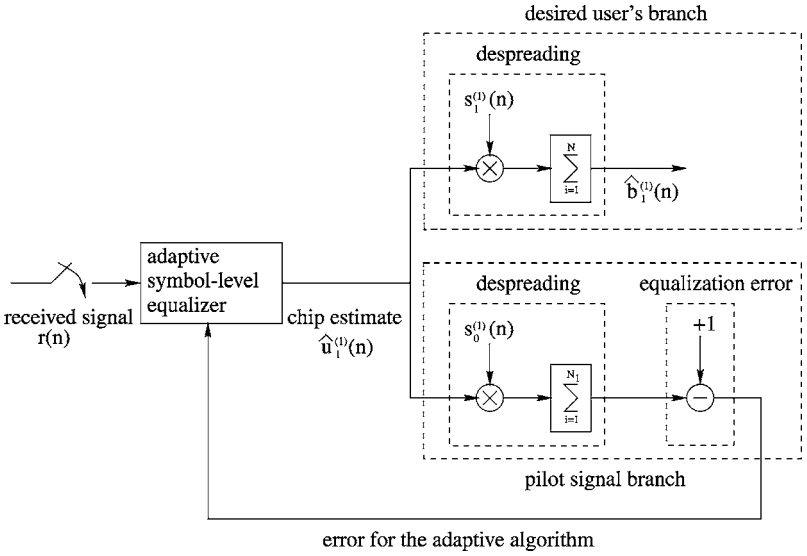

Figure 4. Conceptual diagram of the adaptive symbol-level equalizer (predespreading implementation).

adaptation and the SIR of the training signal. In fast fading channels, it may be desirable to adapt the equalizer multiple times per symbol which is accomplished by setting $N_1 < N$. However, this leads to a lower SIR in the post-despread training signal. Conversely, in static channels, it may be more appropriate to set $N_1 \geq N$. Numerical simulations of the proposed symbol-level adaptive equalizer in time-varying and static channel conditions are presented in Section 5.

Finally, note that, unlike the matched filter receiver and equalizers based on the exact computation of the MMSE solution, the adaptive equalizer does not require any explicit estimation of channel parameters. In particular, the adaptive equalizer requires only coarse timing information in order to capture the energy from the desired chip in its observation window. Provided that the equalizer spans a sufficiently long observation window, the equalizer is robust against timing uncertainty and is capable of tracking timing variations.

4.2. *Average SIR Expressions and Comparison with RAKE Receiver*

The instantaneous SIR attained by the optimum time-varying symbol-level equalizer for the j-th symbol of the desired user is given by (11) with $\mathbf{\Gamma}_1^{(1)}(j)$ and $\boldsymbol{\nu}_1^{(1)}(j)$ substituted in place of $\mathbf{\Theta}(n)$ and $\boldsymbol{\mu}_1^{(1)}(n)$. Following the definition of the average SIR for the average chip equalizer, we define an average SIR for the average symbol-level equalizer as follows

$$\overline{SIR}_{symbol}^{MMSE} \equiv \frac{\left|\left(\bar{\mathbf{p}}_1^{(1)}\right)^H \bar{\boldsymbol{\nu}}_1^{(1)}\right|^2}{\left(\bar{\mathbf{p}}_1^{(1)}\right)^H \bar{\mathbf{\Gamma}}_1^{(1)} \bar{\mathbf{p}}_1^{(1)} - \left|\left(\bar{\mathbf{p}}_1^{(1)}\right)^H \bar{\boldsymbol{\nu}}_1^{(1)}\right|^2} = \frac{\left(\bar{\boldsymbol{\nu}}_1^{(1)}\right)^H \left(\bar{\mathbf{\Gamma}}_1^{(1)}\right)^{-1} \bar{\boldsymbol{\nu}}_1^{(1)}}{1 - \left(\bar{\boldsymbol{\nu}}_1^{(1)}\right)^H \left(\bar{\mathbf{\Gamma}}_1^{(1)}\right)^{-1} \bar{\boldsymbol{\nu}}_1^{(1)}} \tag{19}$$

where $\bar{\mathbf{p}}_1^{(1)}$ is defined in (14). Consider now the average SIR of the RAKE receiver. RAKE reception is a standard demodulation structure for direct sequence systems operating in frequency selective channels. In general, the RAKE receiver can be viewed as a filter matched to the convolution of the chip waveform with the channel, followed by the despreading operation. For the discrete-time chip-synchronous channel model adopted here, the matched filter for the transmission from the first base station is simply the conjugate of the channel $\mathbf{h}^{(1)}$, which is a scalar multiple of the conjugate of the average mean vector $\bar{\boldsymbol{\nu}}_1^{(1)}$. Substituting $\bar{\boldsymbol{\nu}}_1^{(1)}$ for $\bar{\mathbf{p}}_1^{(1)}$ in (19), the average SIR attained by the RAKE receiver for the desired user is given by

$$\overline{SIR}_{symbol}^{RAKE} = \frac{\left(\left\|\bar{\boldsymbol{\nu}}_1^{(1)}\right\|^2\right)^2}{\left(\bar{\boldsymbol{\nu}}_1^{(1)}\right)^H \bar{\mathbf{\Gamma}}_1^{(1)} \bar{\boldsymbol{\nu}}_1^{(1)} - \left(\left\|\bar{\boldsymbol{\nu}}_1^{(1)}\right\|^2\right)^2}$$

where $\|\mathbf{a}\|^2 = \mathbf{a}^H \mathbf{a}$. As is well known, linear MMSE equalizers attain the highest SIR among all linear receivers. In particular, it is always true that

$$\overline{SIR}_{symbol}^{MMSE} \geq \overline{SIR}_{symbol}^{RAKE}$$

4.2.1. *Comparison for Orthogonal Spreading Sequences.*

For the orthogonal spreading model, expressions for the $\overline{SIR}_{symbol}^{RAKE}$ and $\overline{SIR}_{symbol}^{MMSE}$ can be simplified even further by using the relationships

$$\bar{\mathbf{\Gamma}}_1^{(1)} = N I_{or} \mathbf{\Omega}^{(1)} + N^2 P_1^{(1)} \mathbf{h}^{(1)} \left(\mathbf{h}^{(1)}\right)^H$$

and

$$\bar{\boldsymbol{\nu}}_1^{(1)} = N \sqrt{P_1^{(1)}}\, \mathbf{h}^{(1)}$$

where $\mathbf{\Omega}^{(1)}$ is defined in (18). Performing the substitutions and using the matrix inversion lemma, we obtain for the orthogonal spreading model

$$\overline{SIR}_{symbol}^{MMSE,O} = N \frac{P_1^{(1)}}{I_{or}} \left(\mathbf{h}^{(1)}\right)^H \left(\mathbf{\Omega}^{(1)}\right)^{-1} \mathbf{h}^{(1)}$$

$$\overline{SIR}_{symbol}^{RAKE,O} = N \frac{P_1^{(1)}}{I_{or}} \frac{\left(\left\|\mathbf{h}^{(1)}\right\|^2\right)^2}{\left(\mathbf{h}^{(1)}\right)^H \mathbf{\Omega}^{(1)} \mathbf{h}^{(1)}}$$

Note that, by virtue of its definition, $\mathbf{\Omega}^{(1)}$ depends only upon I_{or}, I_{oc}, noise power spectral density N_0 and the channels $\mathbf{h}^{(1)}$, $\mathbf{h}^{(2)}$. Hence, the average SIR performance gain of the equalizer over the RAKE receiver, defined as the ratio of the corresponding SIRs, is independent of the individual user parameters, such as user power, and only depends upon the overall system parameters: I_{or}, I_{oc}, N_0 and the channels. Thus, even in a heavily loaded system using orthogonal spreading sequences in which the desired signal to interference ratio is quite low, the gains achievable through the use of the MMSE average symbol-level equalizer are not diminished, unlike the case of single-user equalization in which the MMSE and matched filter receivers coincide at low signal-to-noise ratios. This desirable feature is validated by the simulation results presented in Section 5.

4.2.2. Comparison for Random Spreading Sequences. For random spreading sequences, using the correlation matrix in (15), the corresponding SIR expressions for the RAKE and the average symbol-level equalizer become

$$\overline{SIR}_{symbol}^{MMSE,R} = \frac{\overline{SIR}_{symbol}^{MMSE,O}}{1 + \frac{1}{N}\left(\frac{I_{or}}{P_1^{(1)}} - 1\right)\overline{SIR}_{symbol}^{MMSE,O}}$$

$$\overline{SIR}_{symbol}^{RAKE,R} = \frac{\overline{SIR}_{symbol}^{RAKE,O}}{1 + \frac{1}{N}\left(\frac{I_{or}}{P_1^{(1)}} - 1\right)\overline{SIR}_{symbol}^{RAKE,O}}$$

where $\overline{SIR}_{symbol}^{MMSE,O}$ and $\overline{SIR}_{symbol}^{MMSE,O}$ are defined above. From these expressions, it follows that

$$\overline{SIR}_{symbol}^{MMSE,R} \geq \overline{SIR}_{symbol}^{RAKE,R}$$

$$\overline{SIR}_{symbol}^{MMSE,O} \geq \overline{SIR}_{symbol}^{MMSE,R}$$

$$\overline{SIR}_{symbol}^{RAKE,O} \geq \overline{SIR}_{symbol}^{RAKE,R}$$

Note also, that as $P_1^{(1)}/I_{or} \to 1$, we have $\overline{SIR}_{symbol}^{RAKE,R} \to \overline{SIR}_{symbol}^{RAKE,O}$ and $\overline{SIR}_{symbol}^{MMSE,R} \to \overline{SIR}_{symbol}^{MMSE,O}$.

Consider now the SIR performance gain of the equalizer relative to the RAKE receiver, given by

$$\frac{\overline{SIR}_{symbol}^{MMSE,R}}{\overline{SIR}_{symbol}^{RAKE,R}} = \frac{\overline{SIR}_{symbol}^{MMSE,O}\left(1 + \frac{1}{N}\left(\frac{I_{or}}{P_1^{(1)}} - 1\right)\overline{SIR}_{symbol}^{RAKE,O}\right)}{\overline{SIR}_{symbol}^{RAKE,O}\left(1 + \frac{1}{N}\left(\frac{I_{or}}{P_1^{(1)}} - 1\right)\overline{SIR}_{symbol}^{MMSE,O}\right)}$$

From this expression, it is apparent that in this case the SIR performance gain does depend upon the individual user parameters through the quantity $P_1^{(1)}/I_{or}$. Furthermore, it is easy to see that (i) the gain is a monotonically increasing function of $P_1^{(1)}/I_{or}$ for all values of $P_1^{(1)}/I_{or}$ (by definition $0 < P_1^{(1)}/I_{or} \leq 1$), (ii) in the limit as $P_1^{(1)}/I_{or} \to 0$, the gain converges to unity. Hence, unlike the case of orthogonal spreading sequences, the gain of the equalizer over the RAKE receiver diminishes to unity as the desired signal to interference ratio decreases when random spreading sequences are used.

4.3. Suppression of Intra-Cell and Other-Cell Interference

For reasons of practicality, only the finite-impulse response MMSE receivers have been considered up to this point. However, some useful insight can be achieved by considering the form of the infinite-impulse response (IIR) implementation of the MMSE equalizer. Let $H^{(1)}(z)$ denote the z-transform of the channel between the serving base station and the desired mobile. Similarly, let $H^{(2)}(z)$ denote the z-transform between the interfering base station and the desired mobile. In general, the other-cell interference spectral density, I_{oc}, and the channel, $H^{(2)}(z)$, can be redefined to include the interference contribution of additive white Gaussian noise of spectral density N_0. Given that the other-cell interference has been redefined in this manner, the z-transform of the average symbol level IIR MMSE equalizer for the DS-CDMA forward link, for both orthogonal and random codes can be shown to be given by

$$\frac{\left(H^{(1)}(z^{-1})\right)^*}{H^{(1)}(z)\left(H^{(1)}(z^{-1})\right)^* + \frac{I_{oc}}{I_{or}}H^{(2)}(z)\left(H^{(2)}(z^{-1})\right)^*} \tag{20}$$

Note that this equalizer is precisely the MMSE equalizer for a non-spread single-user system in which the energy per symbol is unity, the channel between the transmitter and the receiver is given by $H^{(1)}(z)$, and the stationary additive interference has power spectrum

$$\frac{I_{oc}}{I_{or}}H^{(2)}(z)\left(H^{(2)}(z^{-1})\right)^*$$

Note that in the expression (20), the ratio of intra-cell to other-cell interference, I_{oc}/I_{or}, takes the place of the noise spectral density, N_0, used in the standard single user MMSE equalization result.

The asymptotic behavior of the average symbol-level IIR MMSE equalizer provides insight into its interference suppression capabilities. Specifically, note that if the other-cell interference is dominant, and thus $I_{oc}/I_{or} \gg 1$, the IIR MMSE equalizer becomes

$$\frac{I_{or}}{I_{oc}}\frac{\left(H^{(1)}(z^{-1})\right)^*}{H^{(2)}(z)\left(H^{(2)}(z^{-1})\right)^*}$$

which is precisely the whitened-matched filter for the single-user problem [15]. Thus, on the forward link, the MMSE equalizer suppresses other-cell interference by first whitening the interference with the

filter $1/H^{(2)}(z)$, and then filtering with matched filter $(H^{(1)}(z^{-1}))^*/(H^{(2)}(z^{-1}))^*$. Note that if the other-cell interference is white, so that $H^{(2)}(z) = 1$, this interference cannot be suppressed, and the IIR MMSE equalizer becomes the matched-filter receiver. For an environment dominated by intra-cell interference, so that $I_{oc}/I_{or} \ll 1$, the IIR MMSE equalizer becomes simply the zero-forcing equalizer, given by

$$\frac{1}{H^{(1)}(z)}$$

and inverts the channel between the serving base-station and the desired user. By inverting the channel $H^{(1)}(z)$, for DS-CDMA systems with orthogonal spreading sequences, the MMSE equalizer restores orthogonality of the spreading sequences and hence completely suppresses the intra-cell interference.

The FIR MMSE equalizer suppresses intra-cell and other-cell interference in similar fashion. Beginning with Eqs. (17) and (18), and using the matrix inversion lemma, the average symbol-level equalizer under both spreading models is given by (within a positive multiplicative constant)

$$\bar{\mathbf{p}}_1^{(1)} = \left(\mathbf{H}^{(1)}\left(\mathbf{H}^{(1)}\right)^H + \frac{I_{oc}}{I_{or}}\mathbf{H}^{(2)}\left(\mathbf{H}^{(2)}\right)^H + \frac{N_0}{I_{or}}\mathbf{I}_{L_1+L_2+1}\right)^{-1}\mathbf{h}^{(1)}$$

In the region where the intra-cell interference is dominant, so that $I_{oc}/I_{or} \ll 1$ and $N_0/I_{or} \ll 1$, the MMSE equalizer is well approximated by the minimum distortion solution, given by

$$\bar{\mathbf{p}}_1^{(1)} = \left(\mathbf{H}^{(1)}\left(\mathbf{H}^{(1)}\right)^H\right)^{-1}\mathbf{h}^{(1)}$$

Unlike the IIR equalizer, the chip-spaced FIR equalizer does not have enough degrees of freedom to completely invert the channel $\mathbf{h}^{(1)}$. In general, this situation can be remedied by perfoming fractionally spaced equalization. In the region where non-white interference dominates, i.e., $I_{oc}/I_{or} \gg 1$, $I_{oc}/I_{or} \gg N_0/I_{or}$, the MMSE equalizer becomes a whitened matched filter given by

$$\bar{\mathbf{p}}_1^{(1)} = \left(\mathbf{H}^{(2)}\left(\mathbf{H}^{(2)}\right)^H\right)^{-1}\mathbf{h}^{(1)}$$

Note that if the other-cell channel $\mathbf{h}^{(2)}$ is a one-path channel, then the whitened matched filter becomes a simple matched filter and no suppression of other-cell interference is possible. Otherwise, the MMSE solution performs suppression of other-cell interference through the whitening operation. Finally, in the region where white noise dominates the interference, the MMSE solution is given by a simple matched filter, and suppression of other-cell interference is not possible. A numerical example illustrating suppression of intra- and other-cell interference can be found in the following section.

5. Simulation Results

In this section, simulation results are presented for the symbol-level receivers introduced in the previous section. Our main interest lies with the performance of the adaptive average symbol-level equalizer implemented as shown in Fig. 4. The performance of both the RAKE receiver, with perfect knowledge of all channel parameters, and the average symbol-level MMSE equalizer, computed analytically according to the solution in (14) with perfect knowledge of all channel parameters, is shown for comparison. The performance of the adaptive receiver is shown only with the RLS adaptation algorithm. The performance of the LMS adaption algorithm was found not to provide any significant gain over that of the RAKE receiver. This is to be expected, since the LMS algorithm exhibits poor performance in time-varying or noisy channels [15].

The orthogonal spreading model with processing gain of $N = 64$ chips per symbol is assumed for the desired base station. The desired cell is loaded with twenty-two users: five equal-power desired users, the pilot, and sixteen equal-power interferers. The pilot allocation is twenty percent of I_{or}, while the power of the desired users is a simulation parameter. The interferers' and desired user's powers are scaled so that I_{or} remains constant. The numerical results are obtained by averaging across the desired users. For all simulations $I_{or} = I_{oc}$ and $N_0 = 0$. Interference due to the second base station is simulated as white Gaussian noise of variance I_{oc} filtered through the other cell channel $\mathbf{h}^{(2)}$. For all simulations, $\mathbf{h}^{(2)}$ is fixed as a two path channel with equal path gains and delay spread of one chip, so that

$$\mathbf{h}^{(2)} = \left[\frac{1}{\sqrt{2}}, \frac{1}{\sqrt{2}}\right]^T \tag{21}$$

For the desired base station, two multipath channels are simulated. First, consider a relatively short channel (normalized for unit energy) with five multipath components given by

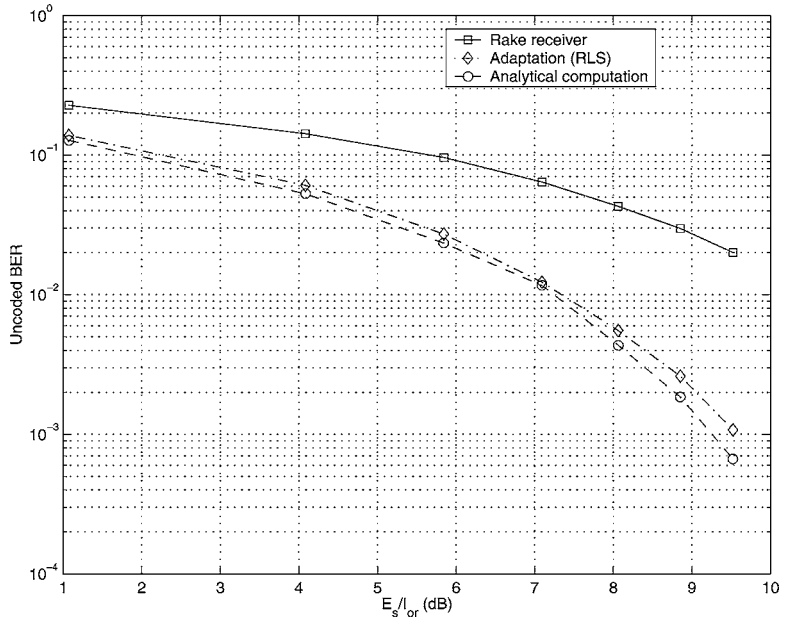

Figure 5. Static channel, $I_{or}/I_{oc} = 1$ (0 dB).

$$\mathbf{h}^{(1)} = \left[\frac{2}{\sqrt{11}}, \frac{1}{\sqrt{11}}, \frac{1}{\sqrt{11}}, \frac{1}{\sqrt{11}}, \frac{2}{\sqrt{11}}\right]^T \tag{22}$$

The length of the equalizer is twice the length of the channel (ten taps in this case). Note that to be consistent with the notation defined in (9), the channel needs to be padded with zeros to be the same length as the equalizer. For the simulations with fading, the channel gains in $\mathbf{h}^{(1)}$ are independently faded using the Rayleigh fading model.

In Fig. 5, the uncoded bit error rate (BER) performance of the three receivers is shown for a static $\mathbf{h}^{(1)}$ versus the ratio of the desired user's symbol energy E_s to the total transmitted power in the desired cell I_{or}, where $E_s = NP_1^{(1)}$. A forgetting factor of 0.98 is used for the RLS algorithm and, since speed of adaptation is not an issue for static channels, the RLS algorithm is updated only once per symbol, i.e. $N_1 = N$. Note that the performance of the adaptive receiver is very close to that of the analytical solution. Furthermore, the adaptive receiver exhibits a significant gain over the RAKE receiver. The gain is independent of the desired user's power, confirming our observation in the previous section that the equalizer gain over the RAKE receiver does not diminish in the region of low $P_1^{(1)}/I_{or}$. In Figs. 6 and 7 performance of the three receivers is shown in fading conditions for Doppler frequencies of $f_D = 10$ Hz and $f_D = 40$ Hz, respectively. Comparing the curves for the static and fading conditions, we note that the performance gains of the adaptive and analytical solutions over the RAKE receiver diminish in fading conditions. In Fig. 7, the performance of the adaptive equalizer with adaptation at both the symbol rate and four times the symbol rate is displayed. At 40 Hz Doppler frequency, the equalizer using symbol rate adaptation does not provide any performance gain over the RAKE receiver. However, adaptation at four times the symbol rate significantly improves the equalizer tracking and results in performance gain over the RAKE receiver in the region of large E_s/I_{or}.

We now consider a longer channel for the desired cell given by

$$\mathbf{h}^{(1)} = \left[\frac{2}{\sqrt{10}}, 0, \frac{1}{\sqrt{10}}, 0, 0, 0, 0, \frac{2}{\sqrt{10}}, \frac{1}{\sqrt{10}}\right]^T. \tag{23}$$

Figures 8, 9, 10 display the performance of the three receivers for $\mathbf{h}^{(1)}$ in static conditions and fading conditions at 10 Hz Doppler frequency and 40 Hz Doppler frequency, respectively. For these simulations, the equalizer has eighteen taps. In static conditions, both adaptive and analytical solutions exhibit a significant performance gain over the RAKE receiver. In comparing Figs. 5 and 8, we note that on the longer channel,

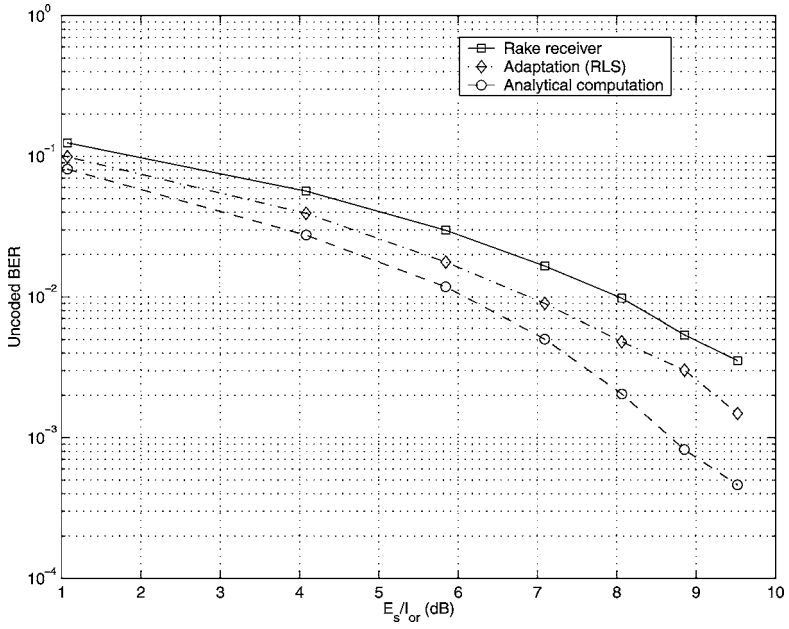

Figure 6. Fading channel: $f_D = 10$ Hz (Normalized Doppler $f_D T = 5.2 \times 10^{-4}$), $I_{or}/I_{oc} = 1$ (0 dB).

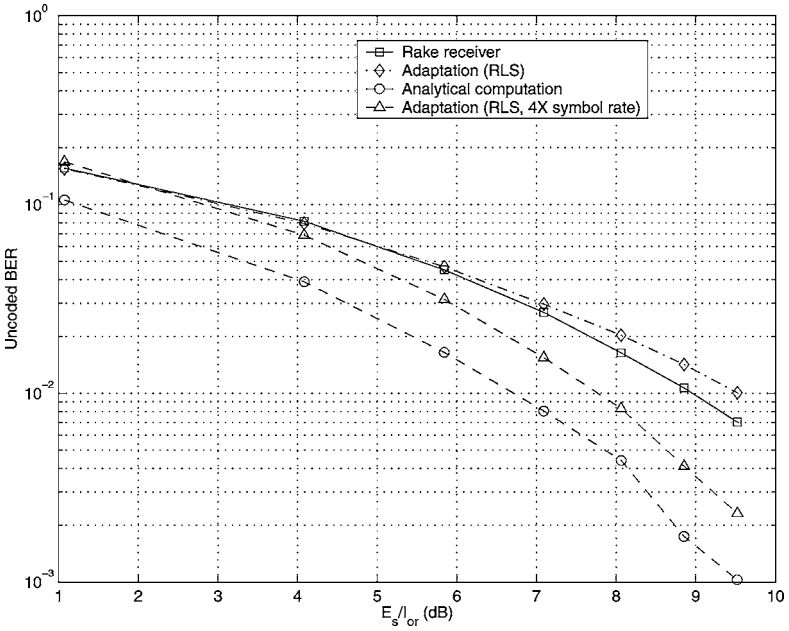

Figure 7. Fading channel: $f_D = 40$ Hz (Normalized Doppler $f_D T = 4.1 \times 10^{-3}$), $I_{or}/I_{oc} = 1$ (0 dB).

the gap between the adaptive and analytical solutions is more pronounced, and this suggests that the steady-state performance of the adaptive algorithm is sensitive to the number of equalizer taps. The observations made based on the fading simulations in Figs. 6 and 7 are further validated by Figs. 9 and 10. In particular, we note that updating the equalizer taps multiple times per symbol helps the tracking performance of the adaptive solution. Nevertheless, the large gap between the analytical and adaptive solutions, as seen in

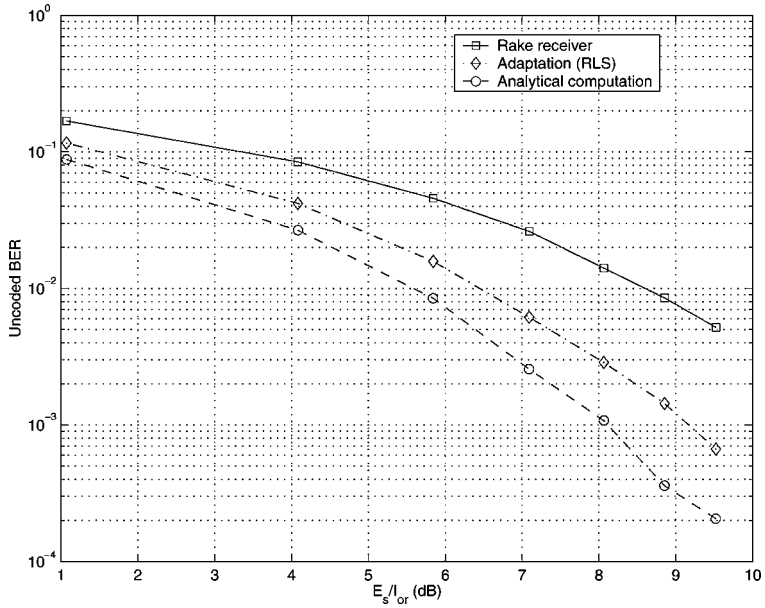

Figure 8. Static channel, $I_{or}/I_{oc} = 1$ (0 dB).

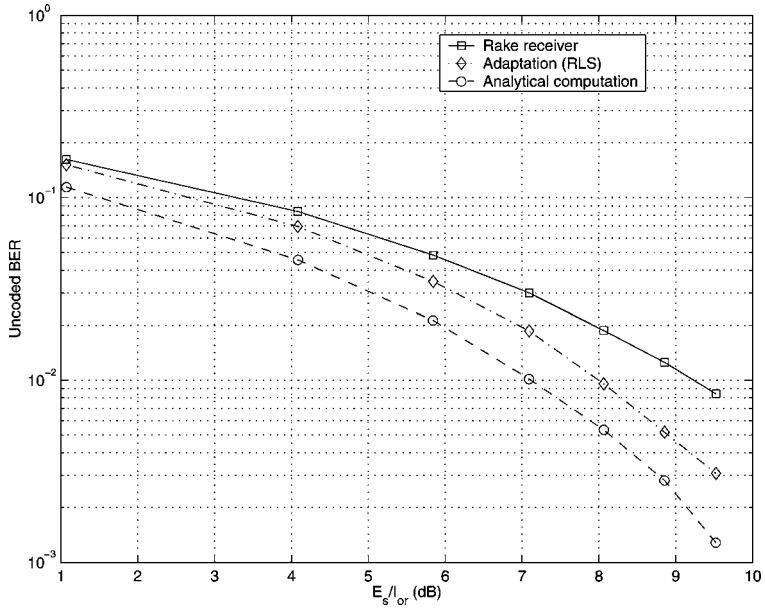

Figure 9. Fading channel: $f_D = 10$ Hz (Normalized Doppler $f_D T = 5.2 \times 10^{-4}$), $I_{or}/I_{oc} = 1$ (0 dB).

Fig. 10, underscores the need for the design of adaptive algorithms which track more accurately.

5.1. Suppression of Intra-Cell and Other-Cell Interference

In Fig. 11, analytical expression for the SIR performance gain of the equalizer over the RAKE receiver is plotted as a function of I_{or}/I_{oc} for orthogonal spreading sequences and channels as above in static conditions. As derived in Section 4.2.1, the gain is given by

$$\frac{\overline{SIR}_{symbol}^{MMSE,O}}{\overline{SIR}_{symbol}^{RAKE,O}} = \frac{\left(\mathbf{h}^{(1)}\right)^H \left(\mathbf{\Omega}^{(1)}\right)^{-1} \mathbf{h}^{(1)} \left(\mathbf{h}^{(1)}\right)^H \mathbf{\Omega}^{(1)} \mathbf{h}^{(1)}}{\left(\left\|\mathbf{h}^{(1)}\right\|^2\right)^2}$$

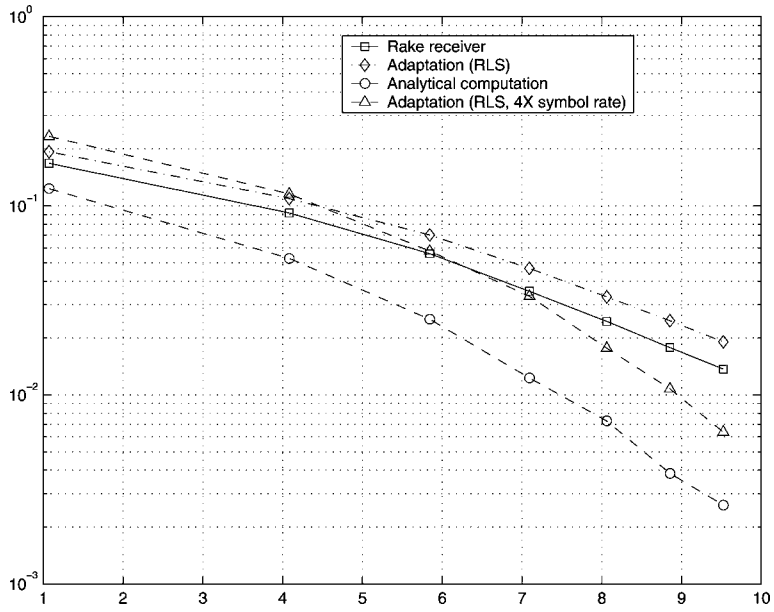

Figure 10. Fading channel: $f_D = 40$ Hz (Normalized Doppler $f_D T = 4.1 \times 10^{-3}$), $I_{or}/I_{oc} = 1$ (0 dB).

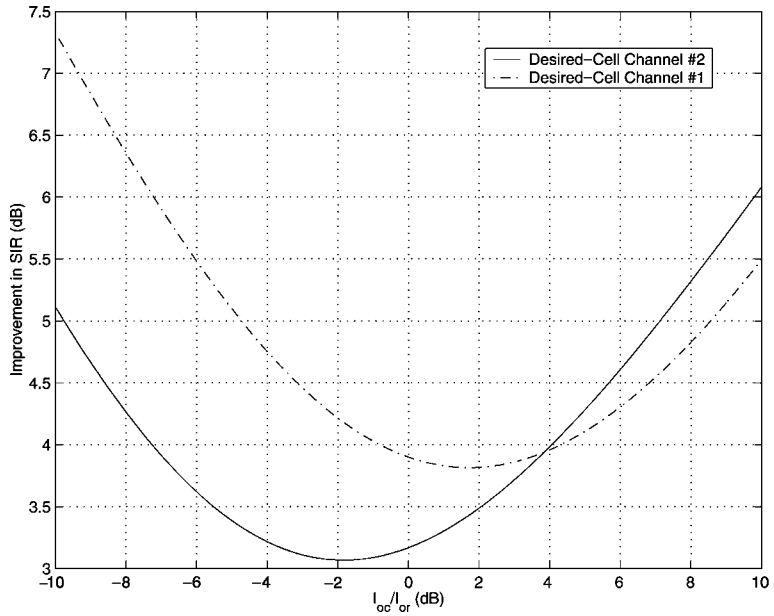

Figure 11. SIR performance gain of the MMSE receiver over the RAKE receiver. Channels 1 and 2 for the desired cell are given by (22) and (23). Other-cell channel is given by (21).

In order to see the limiting performance of the equalizer as the number of taps grows large, we consider an example in which the equalizer has 100 taps. From Fig. 11, it is apparent that the equalizer offers a significant performance gain in SIR over the RAKE receiver over the entire range of interest of I_{or}/I_{oc}. In this example, the largest gains occur if either the other-cell interference or the intra-cell interference is dominant.

6. Conclusions

Linear MMSE equalization at the mobile can significantly improve the performance of DS-CDMA systems that assign orthogonal codes to the users on the forward link. The MMSE equalizer suppresses intra-cell interference introduced by a multipath channel by inverting the channel and restoring code orthogonality. The linear MMSE equalizer can suppress interference from other-cells by whitening the interference. The benefits of other-cell interference suppression apply to CDMA systems with both orthogonal codes and random codes. Other-cell interference is often non-white because the interference from each base station can be modeled as the output of a white source that has been filtered by the channel between the base station and the subscriber. For mobiles in environments dominated by other-cell interference, the MMSE equalizer becomes a whitened-matched filter.

Typically, direct implementation of the MMSE equalizer requires knowledge of the channel between the base-station and the mobile, the covariance of the other-cell interference, and the relative strengths of the intra-cell and other-cell interference. Furthermore, given this information, calculation of the MMSE equalizer is a computationally difficult task. This paper introduces a practical adaptive implementation of the MMSE equalizer for the DS-CDMA forward link, which adapts using the pilot code already present in commercial DS-CDMA systems such as IS-95 and its derivatives. The basic version of the adaptation algorithm presented here and introduced in [3] updates at the symbol rate and measures the pilot error after the received signal has been despread and correlated with the pilot code. In general, chip-rate adaptation of the MMSE equalizer will not perform adequately because the signal-to-noise ratio of the pilot signal prior to despreading and correlation with the pilot code is typically very low.

Acknowledgments

The authors would like to thank Motorola Labs for supporting this work and allowing its publication.

References

1. A. Klein, "Data Detection Algorithms Specially Designed for the Downlink of CDMA Mobile Radio Systems," in *Proc. IEEE International Vehicular Technology Conference*, VTC'97, Phoenix, AZ, May 1997, pp. 203–207.
2. G.E. Bottomley, "Optimizing the RAKE Receiver for the CDMA Downlink," in *Proc. IEEE International Vehicular Technology Conference*, VTC'93, 1993, pp. 742–745.
3. C.D. Frank and E. Visotsky, "Adaptive Interference Suppression for Direct-Sequence CDMA Systems with Long Spreading Codes," in *Proc. 36th Annual Allerton Conference on Communication, Control and Computing*, Monticello, IL, Sept. 1998.
4. I. Ghauri and D.T.M. Slock, "Linear Receivers for the DS-CDMA Downlink Exploiting Orthogonality of Spreading Sequences," in *Proc. 32nd Asilomar Conference on Signals, Systems and Computers*, Asilomar, CA, Nov. 1998, pp. 650–654.
5. S. Werner and J. Lilleberg, "Downlink Channel Decorrelation in CDMA Systems with Long Codes," in *Proc. IEEE International Vehicular Technology Conference*, VTC'99, Houston, TX, May 1999, pp. 1614–1617.
6. M.J. Heikkilä, P. Komulainen, and J. Lilleberg, "Interference Suppression in CDMA Downlink Through Adaptive Channel Equalization," in *Proc. IEEE International Vehicular Technology Conference*, VTC'99—Fall, Amsterdam, Netherlands, Sept. 1999, pp. 978–982.
7. P. Komulainen, M.J. Heikkilä, and J. Lilleberg, "Adaptive Channel Equalization and Interference Suppression for CDMA Downlink," in *Proc. IEEE 6th International Symposium on Spread-Spectrum Techniques and Applications*, ISSSTA 2000, NJ, Sept. 2000, pp. 363–367.
8. T.P. Krauss and M.D. Zoltowski, "Chip-Level MMSE Equalization at the Edge of the Cell," in *Proc. IEEE Wireless Communications and Networking Conference*, WCNC 2000, Chicago, IL, Sept. 2000, pp. 23–28.
9. K. Hooli, M. Latva-aho, and M. Juntti, "Multiple Access Interference Suppression with Linear Chip Equalizers in WCDMA Downlink Receivers," in *Proc. IEEE Global Telecommunications Conference*, Globecom, Rio de Janeiro, Brazil, Dec. 1999, pp. 467–471.
10. F. Petre, M. Moonen, M. Engels, B. Gyselinckx, and H.D. Man, "Pilot-Aided Adaptive Chip Equalizer Receiver for Interference Suppression in DS-CDMA Forward Link," in *Proc. IEEE International Vehicular Technology Conference*, VTC—Fall, Boston, MA, Sept. 2000.
11. G.E. Bottomley, T. Ottosson, and Y.E. Wang, "A Generalized RAKE Receiver for Interference Suppression," *IEEE Journal on Selected Areas in Communications*, vol. 18, Aug. 2000, pp. 1536–1545.
12. S. Chowdury, M.D. Zoltowski, and J.S. Goldstein, "Reduced-Rank Adaptive MMSE Equalization for High-Speed CDMA Forward Link with Sparse Multipath Channels," in *Proc. 38th Annual Allerton Conference on Communication, Control and Computing*, Monticello, IL, Sept. 2000.
13. U. Madhow and M. Honig, "MMSE Interference Suppression for Direct-Sequence Spread Spectrum CDMA," *IEEE Transactions on Communications*, vol. 32, Dec. 1994, pp. 3178–3188.
14. S. Haykin, *Adaptive Filter Theory*, Englewood Cliff, NJ: Prentice Hall, 1996.
15. J.G. Proakis, *Digital Communications*, New York, NY: McGraw-Hill, 1995.

Colin D. Frank received the B.S. degree from the Massachusetts Institute of Technology and the M.S. and Ph.D. degrees from the University of Illinois, all in Electrical Engineering.

He was with the Space and Communications Group of the Hughes Aircraft Company (now Boeing) in El Segundo California from 1983 to 1985. While at the University of Illinois, he served as a consultant for ITT Aerospace and Techno-Sciences, Inc. He joined Motorola Labs in 1993 and is currently with Motorola Systems Sector. For the past 8 years, his work has focused on technology and product development for CDMA systems. His current research interests are in the general area of communication system design and analysis with emphasis on the application of modulation and coding theory to wideband wireless systems. Dr. Frank holds 9 U.S. patents and has published over 20 journal and conference articles.
ACF002@email.mot.com

Eugene Visotsky received bachelor's degree in electrical engineering in 1995, M.S. degree in electrical engineering in 1997, and Ph.D. degree in 2000, all from the University of Illinois at Urbana-Champaign.

He joined the Communication Systems and Research Lab, Motorola Labs, Schaumburg, IL, in 2000. His current research interests are in the areas of wireless communications, multiuser detection, interference suppression, and space-time processing.
visotsky@labs.mot.com

Upamanyu Madhow received his bachelor's degree in electrical engineering from the Indian Institute of Technology, Kanpur, in 1985. He received the M.S. and Ph.D. degrees in electrical engineering from the University of Illinois, Urbana-Champaign in 1987 and 1990, respectively.

From 1990 to 1991, he was a Visiting Assistant Professor at the University of Illinois. From 1991 to 1994, he was a research scientist at Bell Communications Research, Morristown, NJ. From 1994 to 1999, he was with the Department of Electrical and Computer Engineering at the University of Illinois, Urbana Champaign, first as an Assistant Professor and, since 1998, as an Associate Professor. Since 1999, he has been an Associate Professor in the Department of Electrical and Computer Engineering at the University of California, Santa Barbara. His research interests are in communication systems and networking, with current emphasis on wireless communications and high speed networks.

Dr. Madhow is a recipient of the NSF CAREER award. He has served as Associate Editor for Spread Spectrum for the IEEE Transactions on Communications, and as Associate Editor for Detection and Estimation for the IEEE Transactions on Information Theory.
madhow@pablo.ece.ucsb.edu